Journal of Photochemistry & Photobiology, B: Biology 229 (2022) 112425

Contents lists available at ScienceDirect

Journal of Photochemistry & Photobiology, B: Biology

journal homepage: www.elsevier.com/locate/jphotobiol

Deuterated polyunsaturated fatty acids inhibit photoirradiation-induced lipid peroxidation in lipid bilayers

A.M. Firsov [a,1], M.S.F. Franco [b,1], D.V. Chistyakov [a], S.V. Goriainov [c], M.G. Sergeeva [a], E. A. Kotova [a], M.A. Fomich [d], A.V. Bekish [d], O.L. Sharko [d], V.V. Shmanai [d], R. Itri [e], M. S. Baptista [b,*], Y.N. Antonenko [a], M.S. Shchepinov [f,*]

[a] Belozersky Institute of Physico-Chemical Biology, Lomonosov Moscow State University, Russia
[b] Biochemistry Department, Institute of Chemistry, University of São Paulo (IQUSP), AV. Professor Lineu Prestes avenue, 748, USP, CEP: 05508-000 São Paulo, Brazil
[c] SREC PFUR Peoples' Friendship University of Russia, Moscow, Russia
[d] Institute of Physical Organic Chemistry, National Academy of Science, Minsk, Belarus
[e] Applied Physics Department, Institute of Physics, University of São Paulo, Rua do Matão, 1371 (217-B.Jafet), Butantã, USP, 05508-090 São Paulo, Brazil
[f] Retrotope, Inc., Los Altos, 94022, CA, USA

ARTICLE INFO

Keywords:
Lipid peroxidation
D-PUFA
PUFA
Membrane
Photosensitized oxidation
α-Tocopherol
Tocopherol-Mediated Peroxidation
Trolox
Synergism
Age-related diseases
AMD
Sun protection
Photodynamic

ABSTRACT

Lipid peroxidation (LPO) plays a key role in many age-related neurodegenerative conditions and other disorders. Light irradiation can initiate LPO through various mechanisms and is of importance in retinal and dermatological pathologies. The introduction of deuterated polyunsaturated fatty acids (D-PUFA) into membrane lipids is a promising approach for protection against LPO. Here, we report the protective effects of D-PUFA against the photodynamically induced LPO, using illumination in the presence of the photosensitizer trisulfonated aluminum phthalocyanine ($AlPcS_3$) in liposomes and giant unilamellar vesicles (GUV), as assessed in four experimental models: 1) sulforhodamine B leakage from liposomes, detected with fluorescence correlation spectroscopy (FCS); 2) formation of diene conjugates in liposomal membranes, measured by absorbance at 234 nm; 3) membrane leakage in GUV assessed by optical phase-contrast intensity observations; 4) UPLC-MS/MS method to detect oxidized linoleic acid (Lin)-derived metabolites. Specifically, in liposomes or GUV containing H-PUFA (dilinoleyl-*sn*-glycero-3-phosphatidylcholine), light irradiation led to an extensive oxidative damage to bilayers. By contrast, no damage was observed in lipid bilayers containing 20% or more D-PUFA (D2-Lin or D10-docosahexanenoic acid). Remarkably, addition of tocopherol increased the dye leakage from liposomes in H-PUFA bilayers compared to photoirradiation alone, signifying tocopherol's pro-oxidant properties. However, in the presence of D-PUFA the opposite effect was observed, whereby adding tocopherol increased the resistance to LPO. These findings suggest a method to augment the protective effects of D-PUFA, which are currently undergoing clinical trials in several neurological and retinal diseases that involve LPO.

1. Introduction

PUFA make up a large fraction of fatty acids in bilayers that surround cells and organelles. Double bonds exert a substantial effect on membrane fluidity and barrier function, while simultaneously rendering PUFA highly susceptible to oxidation by reactive oxygen species (ROS).

Non-enzymatic lipid peroxidation (LPO) of PUFA and ensuing membrane damage are typical consequences of aerobic metabolism. Under physiological conditions, background level of LPO affects cell signaling, maturation, differentiation, and apoptosis [1]. Pathophysiological increases in LPO are implicated in numerous neurodegenerative, cardiovascular and retinal conditions [2].

Abbreviations: LPO, Lipid peroxidation; D-PUFA, Deuterated Polyunsaturated Fatty Acids; $AlPcS_3$, Trisulfonated Aluminum Phthalocyanine; GUV, Giant Unilamellar Vesicles; FCS, Fluorescence Correlation Spectroscopy; LOOH, Lipid Hydroperoxides; LUV, Large Unilamellar Vesicles; H-Lin-PC, 1-stearoyl-2-linoleoyl-sn-glycero-3-phosphocholine; H-DHA-PC, 1-stearoyl-2-docosahexaenoyl-sn-glycero-3-phosphocholine; D_{10}-DHA-PC, 1-stearoyl-2-(6,6,9,9,12,12,15,15,18,18-D10-docosahexaenoyl)-sn-glycero-3- phosphatidylcholine; D_2-Lin-PC, 1-stearoyl-2-(11,11-D2-linoleyl)-sn-glycero-3-phosphatidylcholine; SRB, sulforhodamine B.

* Corresponding author.
E-mail addresses: baptista@iq.usp.br (M.S. Baptista), shchepa65@yahoo.com (M.S. Shchepinov).

[1] Both authors contributed equally to the work and shall be considered first authors.

https://doi.org/10.1016/j.jphotobiol.2022.112425
Received 12 November 2021; Received in revised form 17 February 2022; Accepted 26 February 2022
Available online 4 March 2022

Generally, LPO involves hydrogen abstraction from the bis-allylic carbons. However, photo-induced LPO initially requires a single double bond, so even a monounsaturated fatty acid can be used at the initiating step [3]. LPO and membrane permeabilization are the hallmarks of light-induced oxidative damage in human skin and are also critical for the elimination of diseased cells in photodynamic therapy (PDT). Combining photosensitizer, light, and oxygen yields ROS that degrade the bilayers [4–9], decreasing their ability to maintain chemical gradients [5–7]. Photoinduced membrane permeabilization (Fig. 1) involves both type I and II mechanisms of photosensitized oxidation. Singlet oxygen ($^1O_2$) adds to double bonds flanked by allylic methylene groups [6], generating lipid hydroperoxides (LOOH) in a process known as the "ene" reaction (Type II mechanism) [3,7]. The formation of LOOH leads to a double bond shift, resulting in an enlarged area occupied per lipid, and increased membrane fluctuations without initially compromising the membrane integrity (i.e. LOOH accumulates in the membrane without causing membrane leakage [8,9]). On the other hand, electron/hydrogen abstraction by the excited state photosensitizer (triplet or singlet excited state) generates carbon-centered free radicals ($L^{\bullet}$, Type I mechanism [1,10], that quickly react with molecular oxygen to form peroxyl ($LOO^{\bullet}$) radicals. $LOO^{\bullet}$ is the main LPO-sustaining species that abstracts neighboring bis-allylic hydrogens, forming another hydroperoxide. Lipid radicals can undergo β-scission yielding lipid truncated aldehydes, which are the main species responsible for membrane leakage [3,11–13].

.

These mechanisms can work in parallel yielding several oxidized products (alcohols, carbonyls, carboxylic acids), and disturb membranes, causing leakage [8,12,14]. The initiation step ($^1O_2$ -"ene" reaction or electron/hydrogen abstraction from alkenes) and the propagation step (hydrogen abstraction by the peroxyl radical) are sensitive to the kinetic isotope effect (KIE) [15–16]. However, whether or not deuterated polyunsaturated fatty acids (D-PUFA) [17,18] (Fig. 2A) can protect against photosensitized oxidation has never been investigated. To evaluate the effects of small amounts of D-PUFA on photo-induced oxidation of H-Lin-PC, we compared the photo-induced LPO in model membranes with and without D-PUFA by fluorescence correlation spectroscopy (monitoring fluorophore leakage) and absorbance at 234 nm (monitoring formation of diene conjugates) in liposomes as well as direct microscopic observation of giant unilamellar vesicles.

Large unilamellar vesicles (LUV) and giant unilamellar vesicles (GUV) are two different membrane mimetic models useful in D-PUFA protection studies [19]. LUV usually range from 100 to 500 nm in diameter, while GUV are larger, at around 1 μm. LUV are more amenable to spectroscopic studies, while GUV are ideal for visual observation under a microscope. In GUV, the effects related to the accumulation of hydroperoxides and lipid truncated aldehydes (Fig. 1) can be separated because the accumulation of hydroperoxides increases membrane fluctuations; the accumulation of lipid truncated aldehydes promotes membrane leakage, as measured by the loss of refractive index contrast between the liquid in GUV lumen and the external media.

The lipophilic antioxidant α-tocopherol is naturally present in lipid membranes, with maximal concentration not exceeding one tocopherol moiety per 10^2–10^3 lipid molecules [2,20]. We also assessed its effect on the D-PUFA-containing bilayer integrity during exposure to light irradiation. Furthermore, we tested Trolox, a water-soluble synthetic analog of tocopherol, to determine the relative importance of antioxidant hydrophobicity for LPO inhibition.

2. Experimental Section

2.1. Materials

1-stearoyl-2-linoleoyl-sn-glycero-3-phosphocholine (H-Lin-PC) and 1-stearoyl-2-docosahexaenoyl-sn-glycero-3-phosphocholine (H-DHA-PC) were from Avanti Polar Lipids, USA.; 1-stearoyl-2-(6,6,9,9,12,12,15,15,18,18-D10-docosahexaenoyl)-sn-glycero-3- phosphatidylcholine (D_{10}-DHA-PC) and 1-stearoyl-2-(11,11-D2-linoleyl)-sn-glycero-3-phosphatidylcholine (D_2-Lin-PC) were manufactured by Retrotope; Al(*III*)Phthalocyanine trisulfonic acid chloride ($AlPcS_3$) was from Frontier Sci, USA. Glucose, sucrose and chloroform were from Sigma Aldrich, Germany. LTB4-d4 (cat.no. 320110), 15-HETE-d8 (cat. no. 334720), 12-HETE-d8 (cat.no. 334570), 5-HETE-d8 (cat.no. 334230) were from Cayman Chemical (Ann Arbor, MI, USA). Milli-Q water (Millipore, France) was used in all experiments.

2.2. Preparation of LUV

Plain and dye-loaded unilamellar LUV were prepared by evaporation under a stream of nitrogen of a 2% solution of a mixture of lipids in chloroform followed by hydration with a buffer solution containing a fluorescent marker for dye-loaded liposomes. We used 5 mg of appropriate phosphatidylcholine mixture and added 0.5 mL of 1 mM sulforhodamine B (SRB) in 100 mM KCl, 10 mM Tris, 10 mM MES, pH 7.4. The mixture was vortexed, passed through several cycles of freezing and

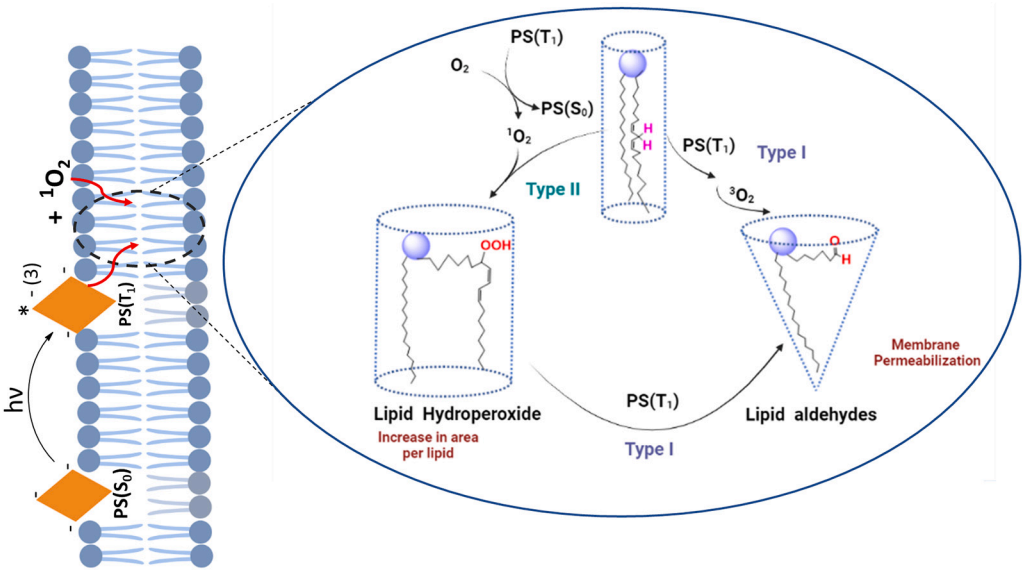

Fig. 1. Chemical steps leading to membrane permeabilization by photosensitized oxidation. Photosensitizer molecules that are bound to the membrane initiate oxidation reactions and generate ROS that diffuse to the inside of the membranes or to the external media. The Type II *contact-independent* mechanism is based on singlet oxygen reaction with lipids. The type I, or *contact-dependent* mechanism comprises radical-mediated pathways by direct contact. $PS(T_1)$: Photosensitizer excited triplet state; $PS(S_0)$: Photosensitizer ground state; $^3O_2$: oxygen ground state; $^1O_2$: Oxygen singlet state. [12]

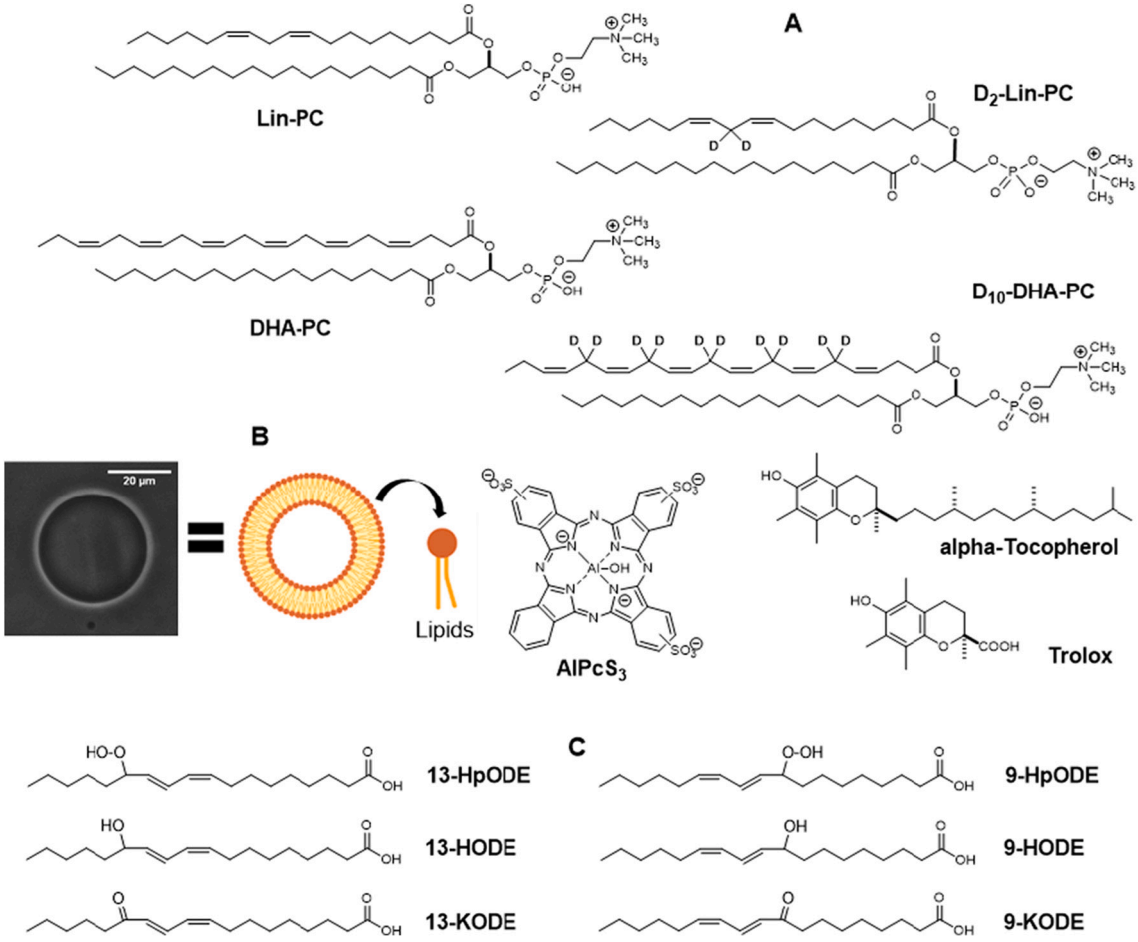

Fig. 2. A, Structures of phospholipids, antioxidants and photosensitizer (Trisulfonated aluminum phthalocyanine) used in this work. B, The bilayer structure of a liposome/GUV. C, Lin-derived oxidation products measured by using UPLC-MS/MS.

thawing, and extruded through 0.1-μm pore size Nucleopore polycarbonate membranes using an Avanti Mini-Extruder. The unbound fluorescent marker was then removed by passage through a Sephadex G-50 coarse column with a buffer solution containing 100 mM KCl, 10 mM Tris, 10 mM MES, pH 7.4.

2.3. Fluorescence Correlation Spectroscopy (FCS)

The custom-made setup was described previously [21]. Briefly, fluorescence excitation and detection utilized a Nd:YAG solid state laser with a 532-nm beam attached to an Olympus IMT-2 epifluorescent inverted microscope equipped with a 40×, NA 1.2 water immersion objective (Carl Zeiss, Jena, Germany). The fluorescence light passed through an appropriate dichroic beam splitter and a long-pass filter and was imaged onto a 50-μm core fiber coupled to an avalanche photodiode (SPCM-AQR-13-FC, PerkinElmer Optoelectronics, Vaudreuil, Quebec, Canada). The output signal was sent to a PC using a fast interface card (Flex02-01D/C, Correlator.com, Bridgewater, NJ). The data were collected under the conditions of stirring liposome dispersions with a paddle-shaped 3-mm plastic bar rotated at 600 rpm. The amplitude of the autocorrelation function at $\tau \rightarrow 0$ ($G(\tau \rightarrow 0)$) is inversely proportional to the number of fluorescent particles $N = 1/G(\tau \rightarrow 0)$, but is independent of the fluorescence intensity of a single particle (in a system of identical particles) and therefore does not depend on the number of fluorophores per vesicle [22]. Particles can be any fluorescent "point objects" in comparison to the linear dimension of the observation volume (i.e. about 1 μm). Therefore, particles can be single molecules of dye (i.e. SRB), as well as liposomes carrying various numbers of dye molecules. Initially (before the leakage induction) the system has a limited number of particles per observation volume comprising predominantly several liposomes loaded with the dye. After the leakage, the number of particles increases substantially, because each liposomal particle produces thousands of particles of free dye leading to a significant decrease in the $G(\tau \rightarrow 0)$ parameter.

2.4. Conjugated Diene Assay

The level of conjugated dienes was determined from the absorption at 234 nm [23]. The UV spectrum of the liposome suspension was measured with a CM 2203 spectrophotometer (SOLAR, Belarus) at various time intervals after the addition of 5 μM $FeSO_4$ and 100 μM ascorbate, subtracting the initial spectrum at time zero. The peak of conjugated dienes was seen as a shoulder in the broad band of ascorbate. As a measure of the level of diene conjugates, the absorbance value at 234 nm was taken, from which the averaged absorbance at 228 nm and 240 nm was subtracted, namely $\Delta A_{234} = A_{234}-(A_{228} + A_{240})/2$. The data points represented Mean ± S.D. of at least three independent experiments.

2.5. Giant Unilamellar Vesicles

Giant unilamellar vesicles (GUV, Fig. 2A) were prepared by electroformation [24]. Lipids were dissolved in chloroform (2 mM) and spread over a conducting face of each of two Fluor Tin Oxide-coated glass slides. The solvent was evaporated and then a 2 mm spacer was placed around the lipid film of one of glass slides and the other one was

used to assemble a chamber. The chamber was filled with 0.2 M sucrose solution and connected to an alternating power generator Minipa MFG-4201A (Korea) at 10 Hz frequency and 1.5 V for 1.5–2 h at room temperature. 100 μL of the GUV were diluted with 0.2 M glucose solution containing $AlPcS_3$ to a final concentration of 1 μM (Fig. 2). Sugar solutions' osmolarities were checked with a cryoscopic osmometer (Osmomat 030 Gonotec, Germany). As controls, photosensitizer-free membranes were continuously irradiated and GUV leakage was detected on the experiment timescale; GUV dispersed in PS-containing glucose solution can be stored safely in the dark.

2.6. Optical Microscopy

The Axiovert 200, Carl Zeiss; Germany, coupled to a Ph2 63 objective was used in this study. Phase contrast mode was used for vesicle observation. The samples were irradiated with the 103 W Hg lamp (HXP 120, Kubler, Carl Zeiss, Germany) applying an appropriate filter for photo activation of $AlPcS_3$ (λ_{ex} = 325–375 nm; beam split 400 nm; λ_{em} = LP 420 nm). Experiments assessing the sugar-induced differences in refractive index resulting in contrast intensity between the GUV interior and surrounding solution, an essential feature for increase membrane permeability [25], were done in triplicate. Optical phase contrast decrease over the time irradiation was analyzed using Image J software, according to the decrease of brightness level intensity. Intensity profiles (6 pixels width) were traced through the vesicle diameter, and the 'Contrast' was defined as the difference between the maximum and the minimum intensity of the profile gray level, as described [25]. The data points represented Mean ± S.D. of at least three independent experiments.

2.7. UPLC-MS/MS Conditions and Sample Preparation

Just after irradiation, the samples were collected and stored at −80 °C for further analysis. Before the solid-phase lipid extraction, solutions were mixed with deuterated internal standard solutions and an equal volume of methanol and centrifuged at 12.000 ×*g* for 5 min (MiniSpin, Eppendorf), the supernatant was mixed with 0.1% acetic acid and loaded onto solid-phase lipid extraction cartridge (Oasis®PRIME HLB cartridge (60 mg, 3 cc)). The cartridge was washed with 2 mL of 15% methanol containing 0.1% formic acid, and the lipids were sequentially eluted with 500 μL of anhydrous methanol and 500 μL of acetonitrile. After the extraction, samples were concentrated by evaporation of the solvent under a gentle stream of nitrogen, reconstituted in 50 μL of 90% methanol and stored at −80 °C for further analysis. For the identification of lipid mediators, the respective lipid extracts were analyzed using an 8040 series UPLC-MS/MS mass spectrometer (Shimadzu, Kyoto, Japan) in multiple-reaction monitoring mode at a unit mass resolution for both the precursor and product ions as described previously [26]. Multiple reaction monitoring (MRM) transitions for metabolites derived from D2-Lin: 9-HpODE (312–185), 13-HpODE (312−113), 9-HODE (296–171), 13-HODE (296–196), 9-KODE (294–185), 13-KODE (294–113). Briefly, the lipid compounds were separated by reverse-phase UPLC (injection volume 20 μL) using Phenomenex C8 column (2.1 mm × 150 mm × 2.6 μm) with the flow rate of 0.4 mL/min. The elution was performed using an acetonitrile gradient in 0.1% (*v*/v) formic acid. The target lipids were identified and quantified by comparing their UPLC, MS, and MS/MS parameters with the respective data obtained for deuterated internal standard compounds employing Lipid Mediator Version 2 software (Shimadzu, Kyoto, Japan).

2.8. Photo-Degradation Control

Solutions containing α-tocopherol at 46 μM in methanol were irradiated as a function of time with a 532 nm Crylass laser (2.1 mW) in the absence and in the presence of $AlPcS_3$ ([$AlPcS_3$] = 1 μM). Absorption spectra (not shown) were obtained at each 3 min of irradiation and had absolutely no variation up to 30 min of irradiation, both in the absence and presence of the photosensitizer. Ultraviolet visible spectra were acquired in 1-cm quartz cells in a Shimadzu UV Visible Spectrophotometer.

3. Results

3.1. Photodynamically-Induced Liposome Leakage

Photodynamic lipid oxidation in GUV can be evaluated by microscopy [27,28]. The formation of lipid hydroperoxides (initial photoproduct of the reaction of the lipid double bond with singlet oxygen) is followed by an increase in the surface area of the membrane, while membrane permeabilization is monitored by the loss of membrane phase contrast (exchange between the sucrose present in GUV lumen and the glucose present in the external medium) (Fig. 2) [29]. Although the hydroperoxidation proceeds quickly, it is not sufficient for the membrane disruption and the leakage, i.e., the phase contrast is preserved while only lipid hydroperoxides are accumulating [9,30,31]. Conversely, light-induced formation of alkoxyl radicals, that progresses through β-scission mechanisms to lipid truncated aldehydes, was shown to induce membrane pores and decrease the GUV phase contrast (Figs. 1 and 2) [31–35]. Here, we have used $AlPcS_3$ as a photosensitizer to induce LPO and membrane damage [36–38].

Effects of $AlPcS_3$ on GUV (Figs. 3 and 4) are monitored through three measurement systems: image evolution (left), area increase (middle) and contrast loss (right). Colour marks in the images (left) are used to represent the respective data points in the graphs. During the first 10 min of irradiation in the presence of $AlPcS_3$, the loss of phase contrast is small (Fig. 3D, H) and it is possible to evaluate the changes in the surface area of the GUV (Fig. 3C, G). Note that there is a substantial increase in the membrane area and in the fluctuations of the GUV made of 100% H-Lin-PC (Fig. 3A, 4 min), but there are no observable changes in the GUV made of 80 mol% of H-Lin-PC and 20 mol% D_2-Lin-PC (Fig. 3B). GUV made of 100 mol% H-Lin-PC show a ~ 30% area increase (Fig. 3C), followed by a similar decrease, which may be due to other factors, including the formation of small membrane buds (not visible in the images). The increase in the surface area is completely prevented by the presence of 20 mol% of D_2-Lin-PC (Fig. 3B). Similar effects were observed in GUV prepared with a mixed composition of lipids (20 mol% of H-DHA-PC and 80 mol% H-Lin-PC), (Fig. 3E, F). Note that the area increase (almost 40%) is greater (Fig. 3E, 8 min) than that observed in the case of GUV made of pure H-Lin-PC (Fig. 3A, 4 min). The replacement of 20 mol% of H-DHA-PC with 20 mol% D_{10}-DHA-PC (Fig. 3F, 8 min), delays the area increase, but does not prevent it (Fig. 3G).

H-Lin-PC GUV showed a considerable loss of contrast during irradiation, indicating membrane leakage. This was prevented by 20 mol% of D_2-Lin-PC (Fig. 3A, D). Likewise, the addition of 20 mol% H-DHA-PC in H-Lin-PC GUV caused a substantial increase in the rate of contrast loss. This was effectively counterbalanced by adding 20 mol% of D_{10}-DHA-PC (Fig. 3F, H). These data demonstrate that D-PUFA efficiently protect against photo-induced membrane leakage in GUV.

The presence of D-PUFA in the H-Lin-PC matrix protected the membrane, (Fig. 3), reducing the contrast loss and the rate of surface area increase, indicative of their capacity to prevent the accumulation of lipid hydroperoxides and the formation of membrane pores by lipid truncated aldehydes. This suggests that D-PUFA (starting at about 20 mol%) inhibit both the initiation and propagation stages of photo-induced LPO [12]. The area increase is a consequence of the accumulation of lipid hydroperoxides on the surface of GUV that occurs mainly as a result of the ene reaction, but also as a result of the $LOO^{\bullet}$-driven hydrogen abstraction from the surrounding PUFA [3]. The fact that H-Lin-PC GUVs prepared with 20 mol% D_2-Lin-PC do not show any level of surface area increase, indicates that D-PUFA efficiently inhibit the accumulation of hydroperoxides. The value of KIE for the ene reaction varies from 1.4 to 2 [39,40], but it is much larger (~10) for the peroxyl-

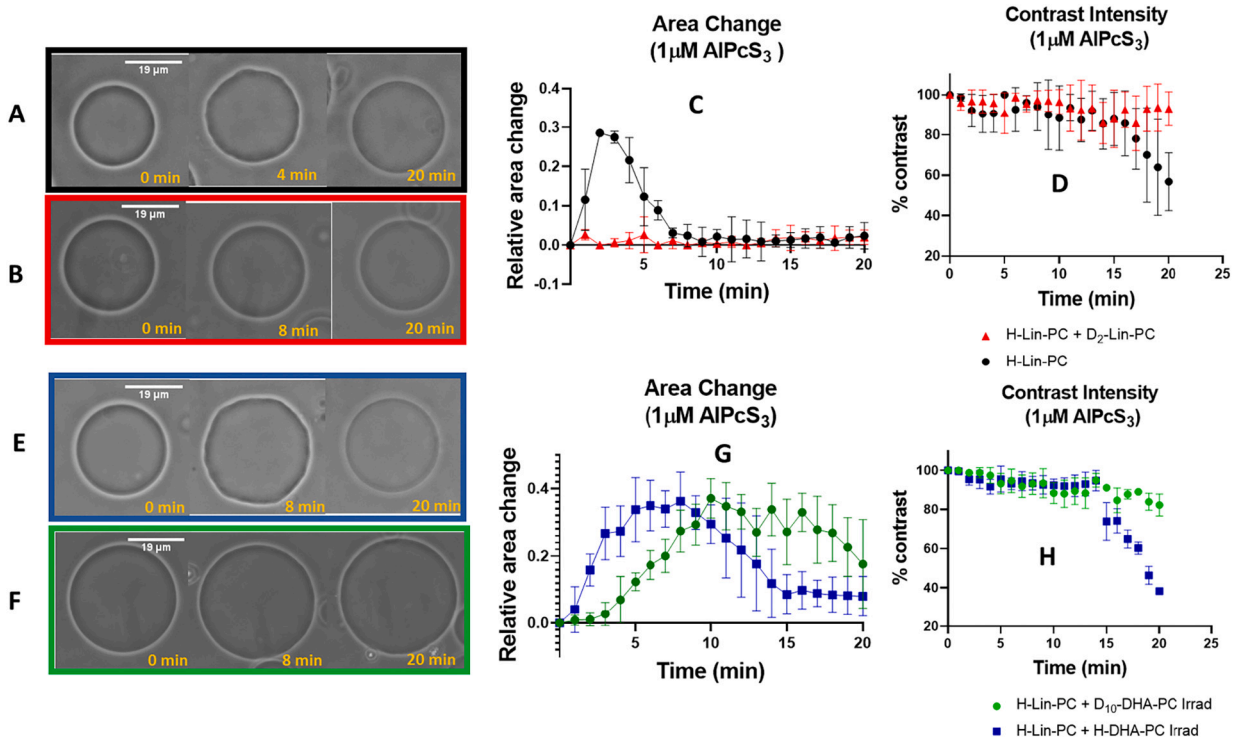

Fig. 3. Phase contrast microscopy images of: A and B, H-Lin-PC (black) and H-Lin-PC + D_2-H-Lin-PC (red); E and F: H-Lin-PC + H-DHA-PC (blue) and H-Lin-PC + D_{10}-DHA-PC (green) in 1 μM $AlPcS_3$ solution at different irradiation times; Morphological changes caused by irradiation of vesicles dispersed in $AlPcS_3$ (1 μM)-containing glucose solution. A, B, E and F show representative pictures of GUV; C and G, changes in the area of the GUV; D and H, changes in GUV contrast, indicative of membrane leakage. The GUV lumen is filled with a sucrose solution. The difference in sugar refractive indexes in the phase contrast model enables the observation by optical microscopy. The irradiation time is shown at the bottom of each snapshot. Each colour corresponds to an experiment with a different GUV lipid composition. (For interpretation of the references to colour in this figure legend, the reader is referred to the web version of this article.)

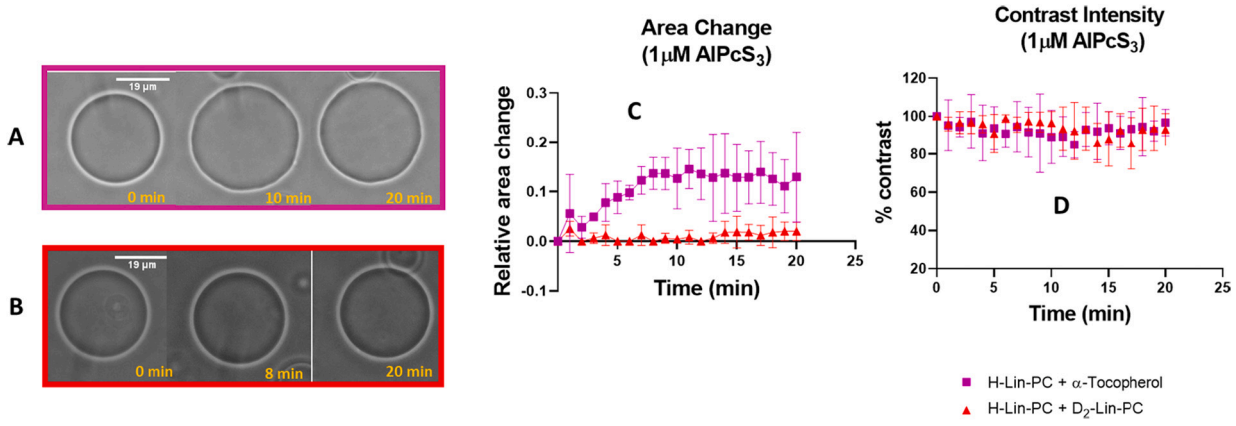

Fig. 4. Representative images of GUV (A, B), changes in the area of GUV (C) and GUV contrast showing membrane leakage (D), H-Lin-PC + D_2-H-Lin-PC and H-Lin-PC + α-tocopherol (Data of H-Lin-PC + D_2-Lin-PC are re-plotted from Fig. 3 to facilitate the visualization). Morphological changes caused by irradiation of vesicles dispersed in $AlPcS_3$ (1 μM)-containing glucose solution. The GUV lumen is filled by a sucrose solution. The difference in sugar refractive indexes in the phase contrast model enables the observation by optical microscopy. The irradiation time is shown at the bottom of each snapshot. Each colour corresponds to an experiment with a different GUV lipid composition.

driven hydrogen atom abstraction [15,41].

Because α-tocopherol is a natural constituent of cellular membranes, it is informative to compare the protection attained with D-PUFA with that of α-tocopherol. GUV made of H-Lin-PC and α-tocopherol (80/20 mol%) were prepared and tested in the same experimental conditions as vesicles containing D-PUFA (Fig. 4) [42]. Tocopherol, like D_2-Lin-PC, inhibited the formation of pores/membrane permeabilization under photo-irradiation, which is noted by the constant levels of phase contrast throughout the experiment (Fig. 4D). However, the same was not true for the area increase. As observed in Fig. 4A, C (purple curve), the presence of 20 mol% of α-tocopherol in H-Lin-PC GUV delayed, but did not completely inhibit, the increase in the surface area. Note the GUV fluctuation and the expansion in surface area of GUV made of 20 mol% α-tocopherol (Fig. 4A), which is not observed in GUV made with 20 mol % of D_2-Lin-PC (Fig. 4B). α-Tocopherol acts as a peroxyl radical-neutralizing antioxidant by donating a hydrogen atom [43]. Therefore, α-tocopherol reacts with oxidation products, inhibiting the outcome of pore formation [44]. Indeed, α-tocopherol turned out to be

as efficient in preventing membrane pore formation as D-PUFA. However, α-tocopherol does not seem to prevent the accumulation of lipid hydroperoxides as efficiently as the D-PUFA. We have performed control experiments that showed the stability of α-tocopherol under the irradiation conditions of our experiments, both in the absence and in the presence of $AlPcS_3$ (data not shown), therefore, the absence of protection recorded in some experiments are not due to the photo-degradation of α-tocopherol. We hypothesized that α-tocopherol can propagate radical chain reaction by a mechanism called Tocopherol-Mediated Peroxidation (TMP), which is based on the bis-allylic hydrogen abstraction by α-tocopherol radical [43,45]. Besides, α-tocopherol is not an efficient scavenger of $^1O_2$, which is the main species responsible for the accumulation of hydroperoxides in the photosensitized lipid oxidation [46]. Therefore, D-PUFA and α-tocopherol exhibit some differences in terms of their mechanism and efficiency of membrane protection against photoinduced oxidation.

We have earlier shown that the fluorescence intensity autocorrelation function (G(τ)) of oxidation-resistant LUV-encapsulated SRB is an efficient method to detect membrane permeabilization by Fe^{2+}/ascorbate-induced oxidation [19,47,48]. The amplitude of G(τ) at the limit τ →0 is determined by the reciprocal of a mean number (N, dye-loaded liposomes) of fluorescent particles in the observation volume under stirring [21,22,49,50]. Fig. 5A shows a time dependence of the G(τ) functions of SRB for liposomes prepared from H-Lin-PC lipid measured without photodynamic treatment (red, green, blue, cyan, dark green lines) and after various light exposures (yellow, pink, green, dark yellow lines). Fig. 5A corresponds to G(τ) upon the addition of Triton-X100 that induces the complete solubilization of lipids and full release of SRB. Illumination of the liposomes led to a decrease in the G(τ→0) amplitude (compare, for example, red and dark yellow lines in 7A). The G(τ→0) values at various periods of illumination (*t*) can be converted into the extent of liposome leakage α using the equation [42]:

$$\alpha(t) = 1 - \sqrt{\frac{G^t(\tau \to 0)}{G^0(\tau \to 0)}} \quad (1)$$

where $G^0(\tau \to 0)$ and $G^t(\tau \to 0)$ represent G(τ) at the limit τ→0 at the moment just before the start of illumination (zero time) and t min of illumination, respectively.

Fig. 5 displays the percentage of integral liposomes during the irradiation time courses in liposomes made of 100% of H-Lin-PC (panel B) or 50% H-Lin-PC and 50% D_2-Lin-PC (panel C). Note that after 5 and 10 min of irradiation, there is a substantial leakage of the liposomes made of 100% of H-Lin-PC (~20% after 5 min and ~ 80% after 10 min of irradiation) while in the presence of 50% of D_2-Lin-PC, there is no significant change after 5-min irradiation and only 30% release after 10-min irradiation (Fig. 5C). As expected, D-PUFA offer good protection against photo-induced membrane leakage.

We have next evaluated the efficiency of α-tocopherol (Fig. 6) in providing membrane protection in liposomes made of 100% of H-Lin-PC (panel A) or 50% H-Lin-PC and 50% D_2-Lin-PC (panel B). Remarkably, α-tocopherol potentiated the SRB leakage in case of 100% H-Lin-PC liposomes (Fig. 6A), thus exhibiting pro-oxidant action under these conditions, which is likely a consequence of the TMP mechanism [43,45]. Note that in liposomes made of 50% H-Lin-PC and 50% D_2-Lin-PC, α-tocopherol increased the level of protection exhibited by D-PUFA. In particular, the leakage from liposomes containing D-PUFA was reduced from 80 to 30% and was further reduced to less than 10% when D-PUFA was supplemented with α-tocopherol (Fig. 6B), suggesting that in the presence of D-PUFA, the TMP mechanism is inactivated.

Interestingly, trolox, a water-soluble derivative of α-tocopherol, exhibited a protective effect at both 100–0% (panel A) and 50–50% (panel B) LUV (Fig. 7). Trolox action occurs mainly in the aqueous media and its membrane-protective effect against photoinduced damage must be related to its ability to scavenge the diffusive photo-induced ROS species, such as superoxide anion radicals and singlet oxygen [51].

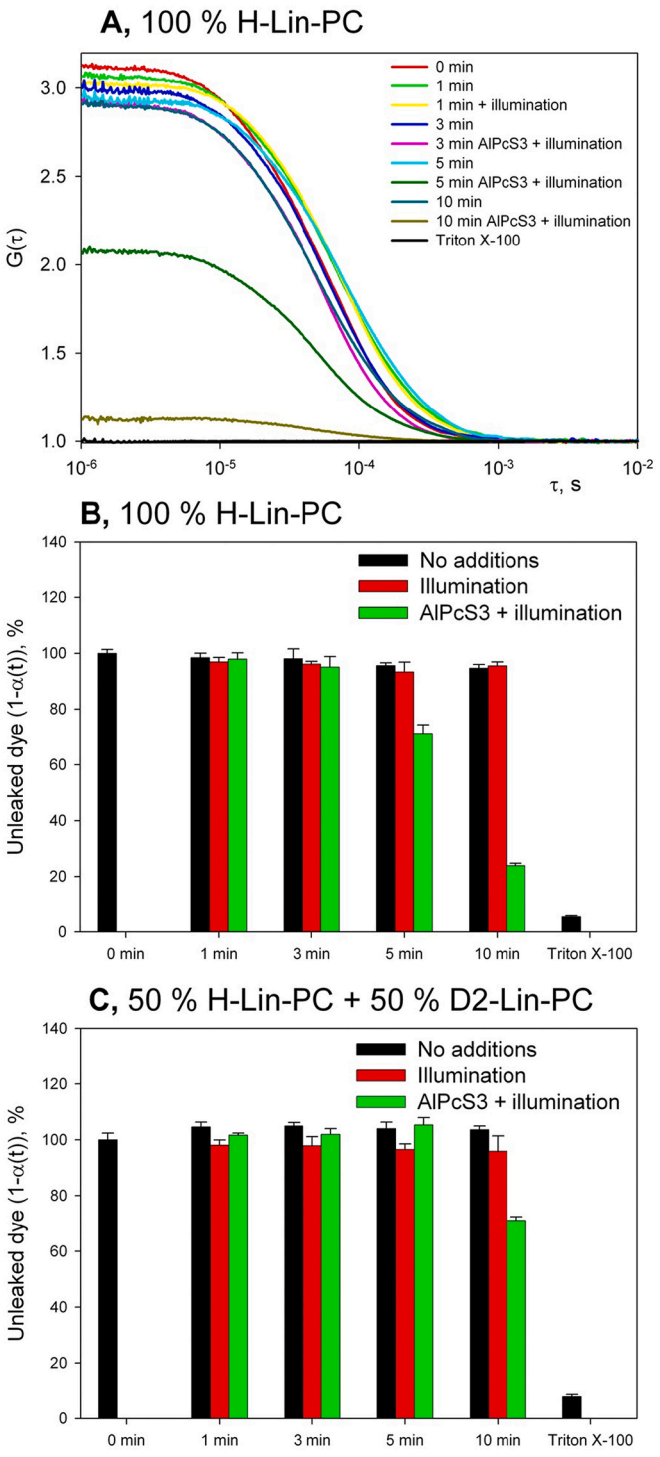

Fig. 5. SRB leakage from large unilamellar liposomes (LUV). A, Typical autocorrelation functions of SRB-loaded H-Lin-PC LUV differing in the time of illumination and the presence of $AlPcS_3$. Autocorrelation function in the presence of Triton-X100 is represented by a black line. The buffer contained 100 mM KCl, 10 mM Tris, 10 mM MES, pH 7.4. Lipid concentration, 10 μg/mL. B,C quantified SRB leakage from 100% H-Lin-PC liposomes.(B) and H-Lin/D2-Lin (1:1)-PC liposomes (C).

3.2. *Downstream Products of the Photo-Induced Membrane Oxidation*

To assess whether or not liposome leakage is associated with LPO, we used the conjugated diene assay, which is based on the measurement of absorption changes at 234 nm (ΔA_{234}), as well as product detection by

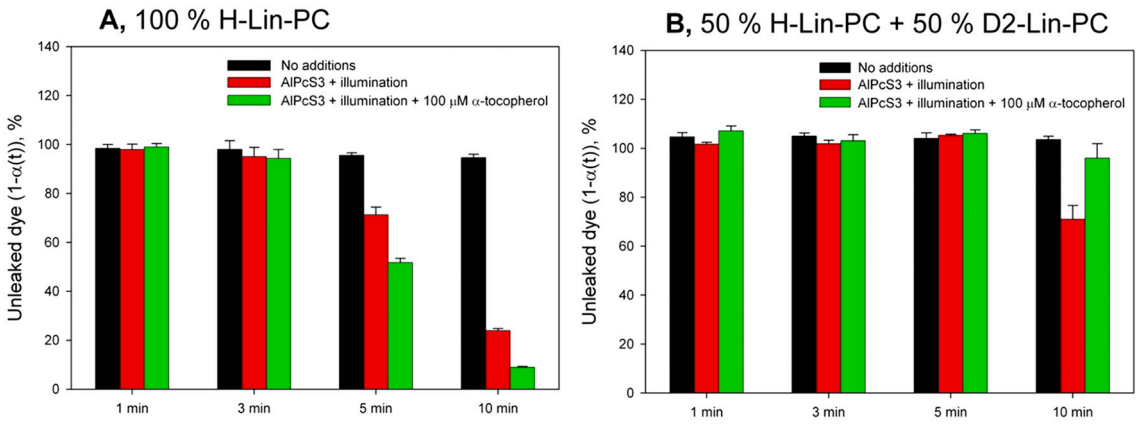

Fig. 6. Effect of tocopherol on the leakage of SRB fluorophore from LUV made of 100% H-Lin-PC (A) or of H-Lin/D_2-Lin (1:1)-PC (B). For experimental conditions see a legend to Fig. 5.

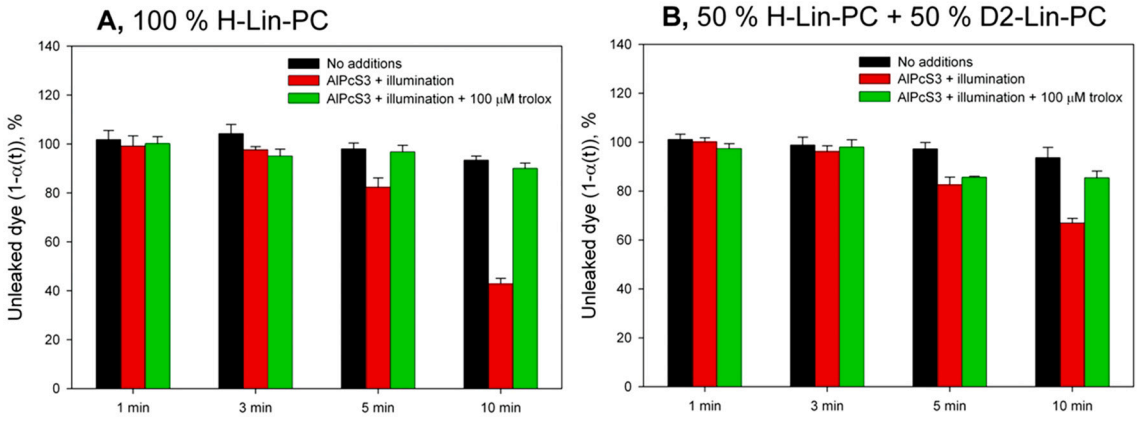

Fig. 7. Effect of trolox on the leakage of SRB fluorophore from LUV made of 100% H-Lin-PC (A) or of H-Lin/D_2-Lin (1:1)-PC (B). For experimental conditions see the legend of Fig. 5.

mass spectrometry [19,23]. In both assays, liposomes were prepared from lipid mixtures containing H-Lin-PC as the bulk lipid (unless otherwise stated) with various contents of 1-stearoyl phosphatidylcholines, bearing D_2-Lin at position 2 of glycerol. Photosensitizer concentration and irradiation protocol were the same as those described above for the liposome leakage experiments.

Fig. 8 shows the absorption changes at 234 nm as a function of irradiation time (panel A) and the UV spectra of liposome (100% H-Lin-PC) suspensions at various irradiation periods (panel B). Note the appearance of a peak in UV spectrum with a maximum at 234 nm, which

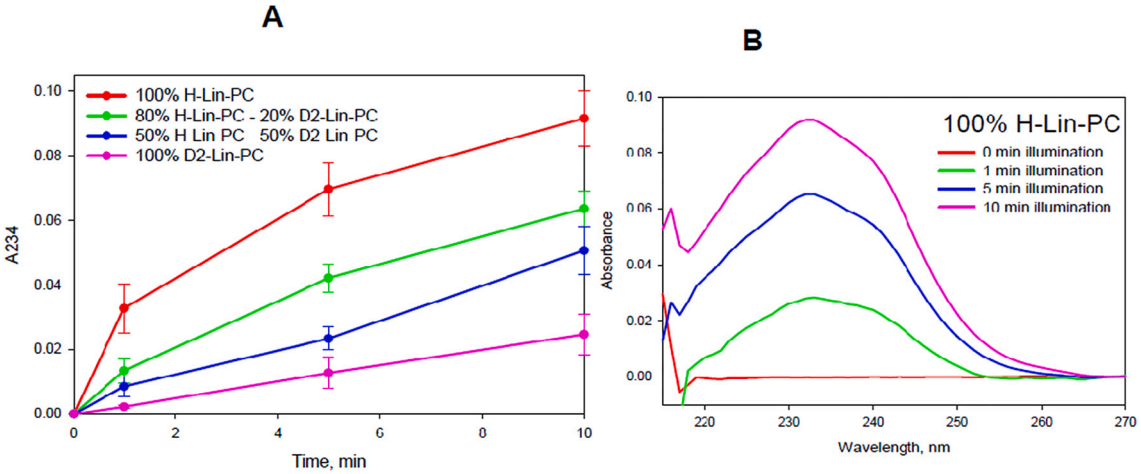

Fig. 8. A. Light induced accumulation of diene conjugates in the presence of 1 μM of $AlPcS_3$ in liposomes with various content of D_2-Lin-PC in H-Lin-PC lipid bilayer. B. Spectra of H-Lin-PC vesicle suspensions under the conditions of red curve on panel A. The buffer contained 100 mM KCl,10 mM Tris,10 mM MES, pH 7.4. Lipid concentration, 10 μg/mL. (For interpretation of the references to colour in this figure legend, the reader is referred to the web version of this article.)

is typical of diene conjugates (Fig. 7B). Note also that with the increase in percentage of D_2-Lin-PC in the liposomal membranes, the ΔA_{234} proportionally decreased, reaching the minimum at 100% of D_2-Lin-PC LUV (Fig. 8A), that represents a higher than 4-fold drop in diene conjugate formation. Importantly, ΔA_{234} values were stable and did not increase in the dark, or in the absence (or after completion) of photodynamic activation (data not shown).

The addition of α-tocopherol to liposomes had negligible effects on ΔA_{234} in the case of 100% H-Lin-PC, while it considerably decreased ΔA_{234} in liposomes made of 50% H-Lin-PC and 50% D_2-Lin-PC (Fig. 9). Similar inhibition of the diene conjugates' formation was observed in case of the addition of 100 μM α-tocopherol in liposomes made of 50% H-Lin-PC and 50% D_2-Lin-PC but not in those made of 100% H-Lin-PC (Fig. 9). The effect was well pronounced 5 min after the start of irradiation (pale blue and pink curves). Lower concentrations of α-tocopherol caused no effect even in the liposomes made of 50% H-Lin-PC and 50% D_2-Lin-PC (Fig. 10). It is evident that the efficiency of membrane protection by 100 μM α-tocopherol increases in the presence of deuterated PUFA, suggesting a possible synergistic enhancement effect.

To detect the products of photodynamic Lin oxidation, we used the UPLC-MS/MS method. LUV were prepared and irradiated as described above. After the experiment, butylated hydroxytoluene was added to the liposomes, and the solution treated with phospholipase A2 from *Vipera ursinii* (a generous gift from Y.N.Utkin, IBCH RAS), for 15 min at 37 °C. Lin-derived metabolites were detected with UPLC-MS/MS (see Material and Methods). After irradiation, the following derivatives of Lin were detected: 9-, 13-HpODE (hydroperoxyoctadecadienoic acid) and 9-, 13-HODE (hydroxyoctadecadienoic acids) (Fig. 11).

When comparing 100% H-Lin-PC and 50/50% H-Lin-PC and D_2-Lin-PC, we observed that the concentration of oxidized metabolites of Lin (9,13-HpODE) is higher in 100% H-Lin-PC liposomes than in 50% deuterated liposomes (Fig. 11A). This is consistent with the results of the A_{234} measurements of diene conjugate formation (Fig. 7). To evaluate the impact of 100 μM α-tocopherol on the oxidation process, we compared the concentration of oxidized Lin-metabolites in 100–0 and 50–50H-Lin-PC and D_2-Lin-PC, in the presence and absence of α-tocopherol. Note that the presence of α-tocopherol decreases 9-HpODE and 13-HpODE in 50/50% D_2-Lin-PC (Fig. 11B), but not in the 100% H-Lin-PC liposomes. Although the decrease in the metabolites with the addition of α-tocopherol is notable, the ratio of H- and D-metabolites does not significantly change with the treatment and consists of approximately 30% of deuterated products both in α-tocopherol treated and non-treated 50/50% D_2-Lin-PC (Fig. 11C). Thus, oxidation is reduced in 50/50% D_2-Lin-PC, relative to 100% H-Lin-PC liposomes, and α-tocopherol additionally reduces the concentration of the oxidized metabolites selectively in 50/50% D_2-Lin-PC liposomes.

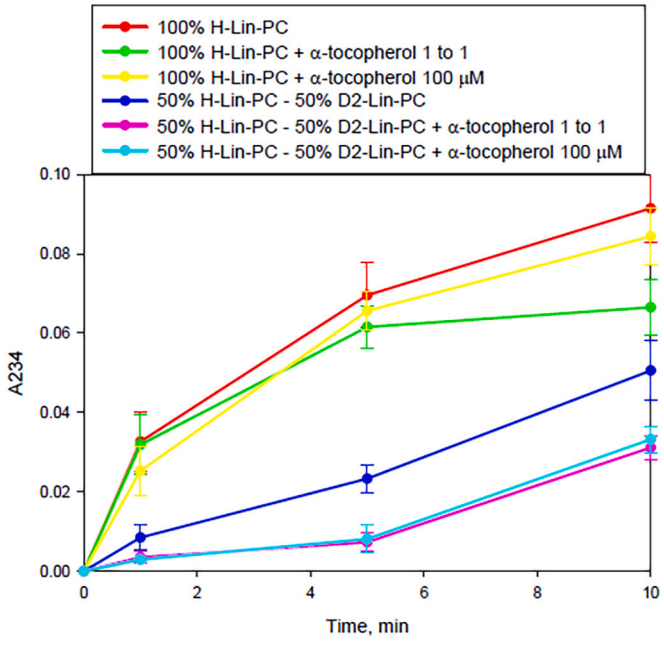

Fig. 9. Effect of tocopherol on the accumulation of diene conjugates in LUV having various contents of D_2-Lin-PC in H-Lin-PC lipid bilayer as a function of illumination with white light in the presence of 1 μM $AlPcS_3$. α-tocopherol was added to the lipid film at the stage of liposome preparation, at the α-tocopherol: lipid ratio of 1:1 (green and pink curves) and at 100 μM concentration (yellow and pale blue curves). (For interpretation of the references to colour in this figure legend, the reader is referred to the web version of this article.)

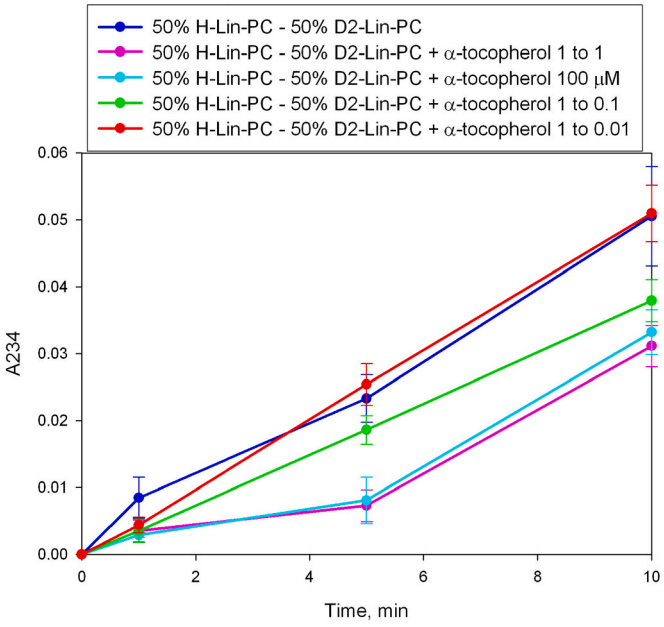

Fig. 10. Dose dependence of the effect of tocopherol on the accumulation of diene conjugates in LUV having 50% D_2-Lin-PC and 50% H-Lin-PC lipid bilayer as a function of illumination with white light in the presence of 1 μM $AlPcS_3$. α-tocopherol was added to the lipid film at the stage of liposome preparation, and at 100 μM concentration (light blue). (For interpretation of the references to colour in this figure legend, the reader is referred to the web version of this article.)

4. Discussion

LPO can be initiated by various ROS capable of abstracting bis-allylic hydrogens, and then proceeds through a chain reaction generating exponential damage [2]. The rate-limiting abstraction step is inhibited by substituting the bis allylic hydrogen atoms with deuterium, inhibiting the LPO process [18,21,52,53]. We have previously established that a relatively small fraction of D-PUFA in lipid bilayers is sufficient to inhibit LPO in liposomes [19] as well as in living cells [54]. Photo-induced oxidation of lipids can occur through the type II singlet oxygen reaction as well as the type I hydrogen abstraction (Fig. 1). Molecules raised to the excited state by photon absorption will have an increased tendency to donate or accept electrons. The magnitude of the pseudo-reduction potentials of the photochemical oxidants in the excited state will basically depend on the energy of the first excited state (lowest vibrational level), which can be estimated by the wavelength of the crossing of the absorbance and fluorescence emission spectra, and on the reduction potential of the molecule in the ground state. Considering that the (0,0) level of the photosensitizer is ~670 nm, giving an increment of 2.3 eV in the reduction potential, and the reduction potential of aluminum phthalocyanines is −0.78 V (SHE), the pseudo-reduction potential of the excited state is 1.5 V. Therefore, the excited state of

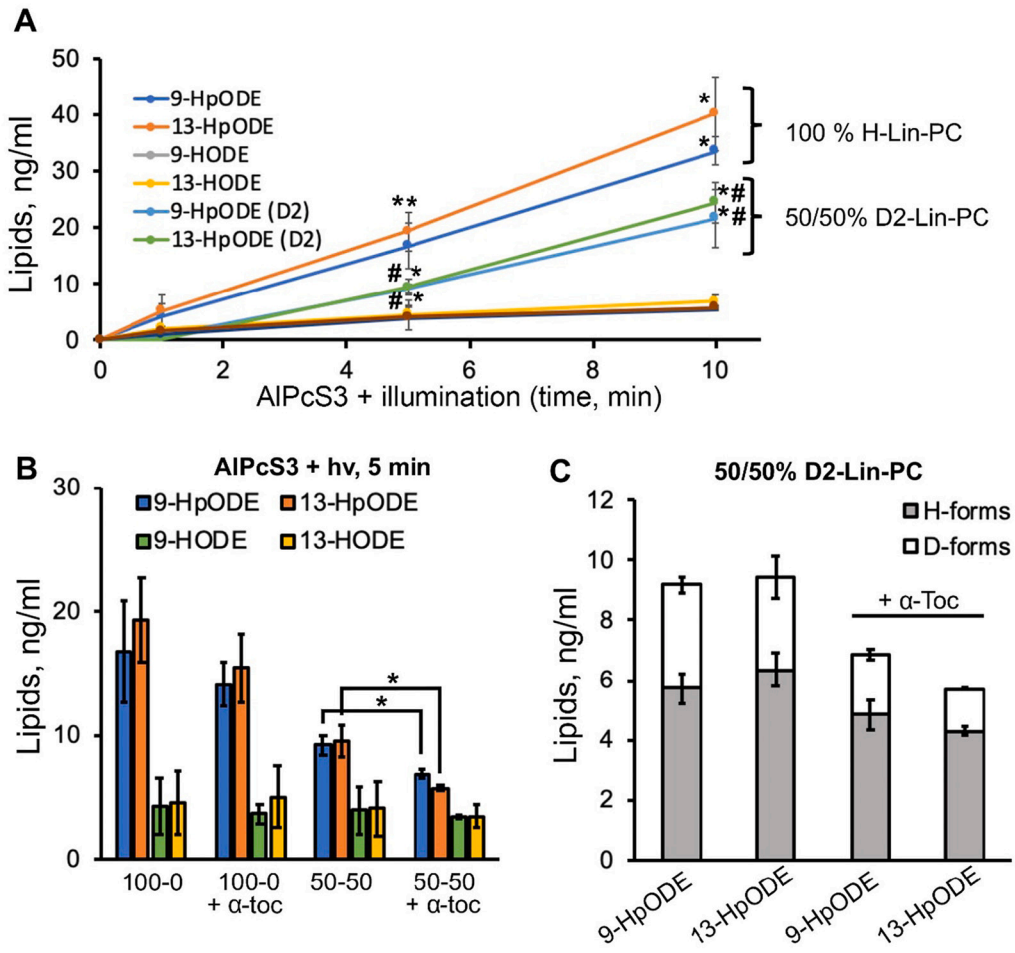

Fig. 11. Effect of α-tocopherol on Lin oxidation products, LUV (100% H-Lin-PC or 50/50% D_2-Lin-PC) were illuminated in the presence of 1 μM of $AlPcS_3$ for 1, 5 or 10 min with or without addition of 100 μM α-tocopherol, and oxidized Lin-derived metabolites were detected using UPLC-MS/MS. A. Concentration of oxidized Lin-metabolites after irradiation. $^*p < 0.05$ compared with non-treated Lin-PC, $\#p < 0.05$ compared with 100% H-Lin-PC B. Effect of α-tocopherol on Lin-derived metabolites concentrations after 5 min of illumination. C. Ratio of oxidized H-(gray) and D-forms (white) of Lin metabolites after 5 min of illumination. The values represent mean ± SD from three independent experiments, $^*p < 0.05$.

the photosensitizer will be capable of abstracting not only the bis-allylic hydrogens from PUFA (PUFA•,H+/ PUFA−H 0.6 V), but also the allylic hydrogens from monounsaturated fatty acids (MUFA, Allyl•,H+/ allyl−H 1.0 V) [55]. Although deuterium substitution has been proven to be very effective in protecting membranes from classical oxidation, this protective effect was never studied under light irradiation conditions.

Based on earlier studies, we chose $AlPcS_3$ as an effective photosensitizer that generates singlet oxygen with a high quantum yield and is stable against photobleaching [56,57]. According to previous data, the binding of $AlPcS_3$ to membranes is a prerequisite for sensitizing both lipid [58] and protein [36,37,59] membrane components to photodamage. We used liposomes (LUV and GUV) made of phospholipids containing H-PUFA and D-PUFA to determine the effect of D-PUFA incorporation on the photodamage resistance of the lipid bilayers, utilizing four experimental systems: 1) optical phase-contrast intensity observations in GUV; 2) sulforhodamine B leakage from LUV, detected with FCS using changes in the amplitude of autocorrelation function; 3) formation of diene conjugates in liposomes, measured by absorbance at 234 nm; 4) quantifying oxidized Lin-derived metabolites using UPLC-MS/MS method. All results confirm the inhibitory effect of D-PUFA on the light-induced lipid bilayer permeabilization and point to synergistic action of D-PUFAs and α-tocopherol.

The presence of 100 μM α-tocopherol potentiated the dye leakage in case of 100–0% LUV (Fig. 6). The addition of α-tocopherol resulted in elevation of LPO in H-PUFA bilayers compared to photoirradiation alone, signifying α-tocopherol's pro-oxidant properties. In this context, the observed Tocopherol-Mediated Peroxidation (TMP Cycle, Fig. 12) resembles a mechanism initiated with formation of an α-tocopherol radical (α-toc•) followed by the propagation of LPO (i), with hydrogen atom abstraction being the rate-limiting step. The lipid-derived radical would then quickly react with abundant oxygen forming lipid peroxyl radicals (L-OO•), that are able to abstract hydrogen off the neighboring intact PUFAs, sustaining the chain reaction of LPO cycle [60]. On the other hand, lipid peroxyl radical react with α-TocH, producing LOOH and regenerate α-Toc•. The TMP cycle, as proposed by Stocker and Bowry, reveals the pro-oxidant mechanism of α-tocopherol, in addition to the possible concomitant oxidation cycle of LPO [45], making H-PUFA LUV highly oxidizable.

In parallel, GUV experiment showed that the presence of α-tocopherol protected liposomes from the sucrose leakage (80% H-Lin-PC + 20% α-tocopherol). The fluctuation and expansion in the surface of GUVs are the fingerprint of hydroperoxide radical formation. In GUV, the α-tocopherol trapped on the membrane-water interface decreases the probability of oxidized lipids to get in contact with the two membrane leaflets and initiate pore formation [44]. This suggests that the pro-oxidant role observed in LUV is due to the relative high concentration of lipid to α-tocopherol (1:10 in the LUV system, compared with 4:1 in GUV system) (Fig. 9).• The presence of D-PUFA in LUV decreases the ROO• formation resulting in the protection against LPO [43]. A protective effect was also observed by the A_{234} assessment of diene conjugate generation (Fig. 7), and by the UPLC-MS/MS detection of Lin oxidation products (Fig. 11). Taken together, the data from these different approaches suggest that tocopherol-induced quenching of photoirradiation-derived lipid radicals is more efficient in the presence of D-PUFA. The replacement of the bis-allylic hydrogen atoms with deuterium arrests PUFA autoxidation due to the isotope effect (Fig. 12) [17,18].

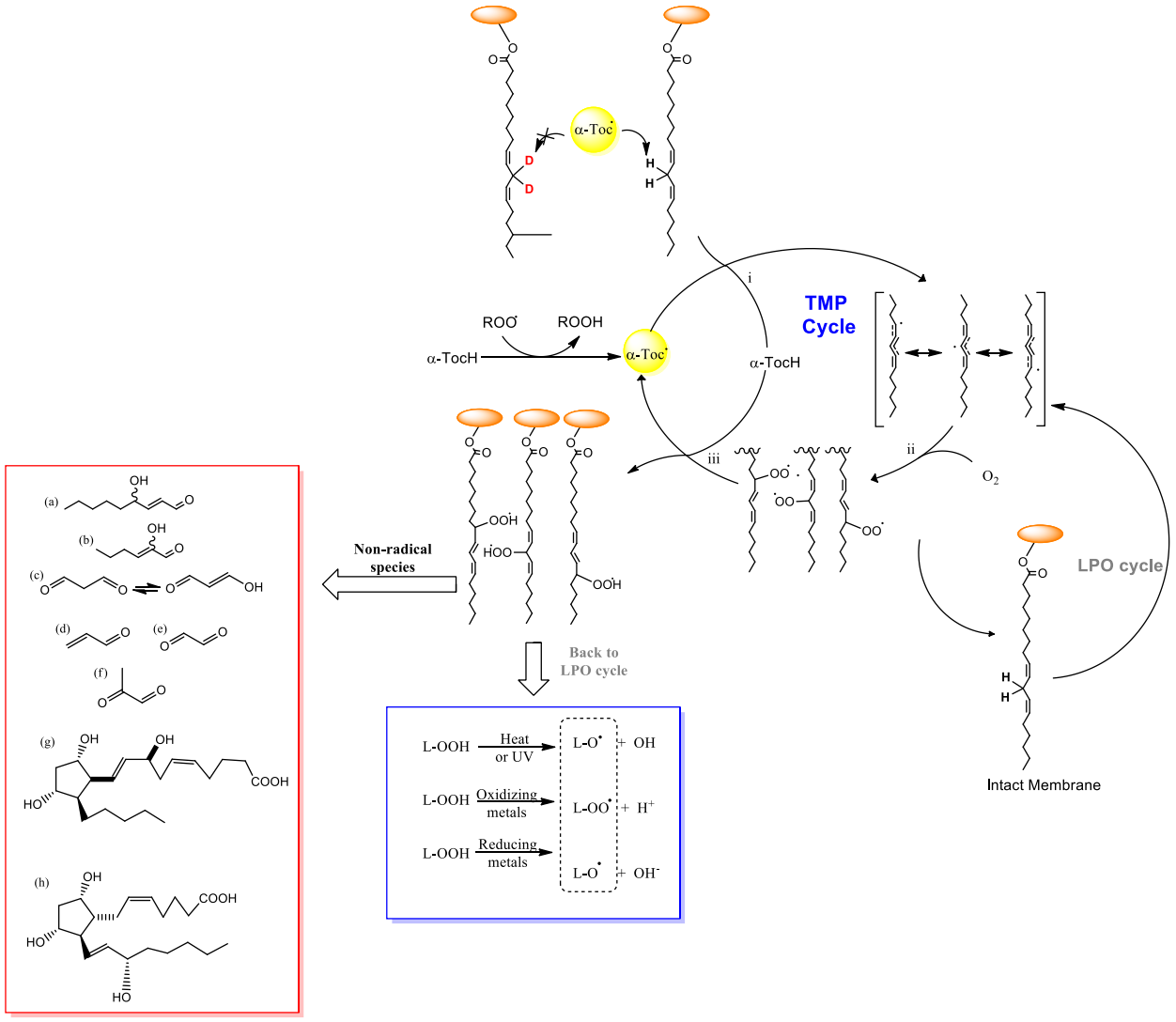

Fig. 12. Tocopherol-mediated Peroxidation (TMP). (i) rate-limiting: hydrogen atom abstraction from LH by α-Toc·; (ii) oxygen addition reaction of L·; (iii) reaction of LOO• + α-TocH = LOOH and regenerate α -Toc·. Peroxides formed may decompose through multiple pathways back into chain-initiating radicals (in blue), which can return to LPO Cycle. However, peroxides can drive to numerous nonradical species (reactive carbonyls), such as: 4-HNE (a), 4-hydroxy-2-hexenal (b), and MDA (in tautomeric form) (c), acrylic aldehyde (d), oxalic aldehyde (e), and methylglyoxal (f). Other classes of products include Ara-derived isoprostanes (g; iPF2α-IV, or 8-F2-IsoP, which is one of 64 different isomers), as well as PGF2α (h), a prostaglandin that can be produced both enzymatically and nonenzymatically. (For interpretation of the references to colour in this figure legend, the reader is referred to the web version of this article.)

To quantitatively evaluate the possible interplay between the lipophilic (α-tocopherol) and hydrophilic (trolox) antioxidants and the presence of D-PUFA in the lipid bilayer, we calculated the independent contributions of the antioxidants and/or deuterated lipids (50% of PUFA) to the protection of the membranes. These were then compared to the findings observed in the presence of both. This calculation is shown in Tables 1–6 for the data obtained by FCS (prevention of liposome leakage, Tables 1–4) and UV spectrophotometry (protection against the accumulation of diene conjugates, Tables 5 and 6) after 10 min of irradiation. As noted previously (Fig. 6), the presence of D-PUFA protects the membrane (note in Table 1, Δ% of membrane leakage decreases from 24.3 to −1.3), while the presence of α-tocopherol increases

Table 1
liposome leakage FCS (data from Figs. 5 and 6) after 10 min irradiation.

% D	Control (Δ%)	α-tocopherol 100 uM (Δ%)
0	24.31	43.85
50	−1.30	−1.99

Table 2
Enhancement calculation from Table 1.

Condition	Δ % (a) Experiment-control	Additivity (b) Expected value	+enhancement/−inhibition (c) Observed –Expected (Δ/Expected) Simple addition
Dienes			
α-toc	−19.54		–
D-50%	+25,61		
Both	+26.21	−6,07	+20.14 (+79%)

(a) Level of membrane damage by calculating the difference of percentage leakage in the liposomes kept in the dark compared with those irradiated in the presence of 100% Lin and 50% deuterated D_2-Lin-PC.
(b) Simple addition of the effects of the presence of 50% D-PUFA and addition of α-tocopherol.
(c) Difference from the expected and experimental values. Positive values are in blue and represent enhancement. Negative values (red) represent inhibition. Percentage values were calculated by dividing the difference (observed-expected) by the expected value.

Table 3
liposome leakage FCS (data from Figs. 5 and 7) after 10 min of irradiation.

% D	Control (Δ%)	Trolox 100 uM (Δ%)
0	50.52	3.62
50	26.69	8.26

Table 4
Enhancement calculation from Table 3.

Condition	Δ % (a) Experiment-control	Additivity (b) Expected value	+enhancement/inhibition (c) Observed –Expected (Δ/Expected) Simple addition
Dienes			
Trolox		+46.9	–
D-50%	+23.83		
Both	+70.73	>100	−14.5 (−15%)

(a) Level of membrane damage by calculating the difference of percentage leakage in the liposomes kept in the dark compared with those irradiated in the presence of 100% Lin and 50% deuterated D2-Lin-PC.
(b) Simple addition of the effects of the presence of 50% D-PUFA and addition of α-tocopherol.
(c) Difference from the expected and experimental values. Positive values are in blue and represent enhancement. Negative values (red) represent inhibition. Percentage values were calculated by dividing the difference (observed-expected) by the expected value.

Table 5
Diene conjugate accumulation (ΔAbsorption from Fig. 9).

% D	Control	α-tocopherol 100 uM
0	0.0696	0.0657
50	0.0233	8.0873e-3

the damage (Δ% of membrane leakage increases from 24.3 to 43.8, Table 1). Remarkably, in the presence of D-PUFA, α-tocopherol is protective (Δ% of membrane leakage decreases from 43.8 to −2, Table 1), with 79% enhancement (Table 2), i.e., with the tocopherol-rendered protection increasing by 79% in the presence of D-PUFA (Tables 5 and 6). D-PUFA alone offer good protection against the accumulation of diene conjugates (ΔAbsorption is reduced from 0.0696 to 0.0233, Table 5). Note that α-tocopherol does not provide any level of protection against the accumulation of diene conjugates in membranes made of 100% H-Lin-PC (ΔAbsorption changes from 0.0696 to 0.0657, Table 5), while α-tocopherol dramatically increases the protection of membranes made of 50% D-PUFA (ΔAbsorption decreases from 0.0657 to 8.1e-3, Table 5) with 37% enhancement (Table 6). Lin-derived metabolites (HpODE and HODE) are produced by LPO [61,62] initially as hydroperoxy-oxydecadienoic acid (HPODE), which is then reduced to HODE [63]. Using UPLC-MS/MS we quantified the accumulation of photoinduced oxidation products in 100% H-Lin-PC or 50/50% D_2-Lin-PC in the presence and absence of α-tocopherol. In the presence of tocopherol, 50/50% H-Lin-PC/D_2-Lin-PC leads to decreased levels of these oxidation derivatives, demonstrating the synergistic protective effect of D-PUFA and α-tocopherol. Interestingly, trolox, which is a hydrophilic analogue of α-tocopherol, acts by neutralizing aqueous soluble oxidant species. Our results show that it protects the membrane mimetic systems investigated here in an almost independent matter of the presence of D-PUFA (Tables 3 and 4). In fact, the level of protection by trolox is more than 4-fold smaller in the membranes made of D-PUFA (Δ% of membrane leakage decreases from 26.7 to 8.26, Table 3) compared to those made of H-Lin-PC alone (Δ% of membrane leakage decreases from 50.5 to 3.62, Table 3), with an antagonism of 15% (Table 4). The failure of D-PUFA to improve the effects of trolox is a direct consequence of the different environments they operate (lipophilic versus hydrophilic), but the exact nature of the observed 15% antagonism requires further investigation.

α-Tocopherol is widely applied as a chain-terminating antioxidant [2,20,60]. However, as mentioned above (Fig. 12), its pro-oxidant role in LDL oxidation has been reported [43,60]. It has also been observed that α-tocopherol can substantially increase the observed KIE values of D-PUFA for oxidation reactions in organic solvent, which requires both close association with D-PUFAs and a hydrogen tunnelling mechanism. Essentially, α-tocopherol acts in synergy with deuterium substitution [53]. Contrarily, trolox does not interact effectively with the lipid bilayer and therefore it does not participate in reactions happening within lipid membranes. However, trolox effectively supresses triplet excited states, singlet oxygen, as well as other ROS such as anion radical superoxide, which can escape the membrane region and migrate to the bulk solution, where trolox will neutralize them [64], preventing their effects on the oxidation of the membranes. The fact that trolox is not bound to the membrane, prevents its participation the TMP pro-oxidative mechanism. Indeed, no pro-oxidation was observed in the presence of Trolox (Fig. 7).

The importance of lipid bilayers in cells cannot be overstated. A perspicacious 1952 adage by Davson and Danielli: “It can truely be said of living cells, that by their membranes ye shall know them”, has been fully corroborated since then [65]. Functionally, for PUFA-rich neurons and mitochondria, lysosomes and retinal outer segments, the most important part of a cell or of an organelle is the lipid membrane. Accordingly, the related pathologies in these cells are often linked to membrane malfunctions. LPO plays a key role in many neurodegenerative (Parkinson’s, Alzheimer’s) and age-related (retinal and skin) pathologies, as well as cancer, atherosclerosis and others diseases, however antioxidants are inefficient for a variety of reasons [2,17]. Light irradiation can initiate LPO through various mechanisms and may be an important tool in understanding oxidative stress diseases.

The use D-PUFA to keep the LPO in check has been recently suggested as a therapeutic strategy [17], because the full protection by D-PUFA is observed even at relatively low (20–30%) threshold level of incorporation into lipid membranes [19], and such a level is quickly

Table 6
Calculation of enhancement.

Condition	Δ % (a) Experiment-control Percentage of protection	Additivity (b) Expected value Simple addition	+enhancement/inhibition (c) Observed –Expected (Δ/Expected)
Diene conjugate			
α-toc	0.0039	–	
D50%	0.0463		
Both	0.06878	0.0502	+0.01858 (+37%)

(a) Percentage of protection. The control of Toc 1:1 and Toc 100 is control 0%. The control of Toc 1:1 and Toc100 in the presence of D10% is Percentage of damage at D 10% (without Toco). The control of Toc 1:1 and Toc 100 in the presence of D50% is Percentage of damage at D 50% (without Toco).
(b) Simple addition of the effects of deuteration and addition of α-tocopherol. Toc 1:1 at 10% D (0.0081 + 0.0298 = 0.0379); Toc 100 at 10%D (0.0039 + 0.00298 = 0.0337); Toc 1:1 at 50% D (0.0081 + 0.0463 = 0.0544); Toc 100 at 50%D (0.0039 + 0.0463 = 0.0502)
(c) Observed is the value in (a) and Expected is the value in (b). Positive values (blue) represent enhancement and negative values (red) represent inhibition. Percentage values were calculated by dividing the difference (observed-expected) by the expected value.

attainable and does not require substantial dietary changes [65–67]. The efficiency of protection depends on the total number of deuterated bis-allylic methylene groups in the lipid bilayer [19,53].

The LPO inhibition and mitigation of disease phenotypes has been described in homogenous solution [53,68], liposomes [19], cells [52,54,69–71] and rodents [67,72,73], as well as in completed and ongoing human studies [66,74], making a good use of this non-linear threshold protection level. Such studies can benefit from additional insights into the mechanism of D-PUFA protection. The data reported herein lends further support to the application of D-PUFA in retinal conditions, in sun-protection strategies, and in liposome-based drug delivery approaches [75], as both the drug vehicles, and the drugs to be delivered.

Disclaimers

M.S.S. is the Chief Scientific Officer of Retrotope, Inc.

Declaration of Competing Interest

The authors declare that they have no known competing financial interests or personal relationships that could have appeared to influence the work reported in this paper.

Acknowledgements

Lipid peroxidation measurements via diene conjugate formation were financially supported by the Russian Science Foundation grant N° 19-74-00015 to A.M.F., liposome leakage experiments by fluorescence correlation spectroscopy were financially supported by the Russian Science Foundation grant N° 21-14-00062 to Y.N.A. The authors are grateful to Dr. Ana Krtolica, Dr. Mark Midei and Dr. Lex Van der Ploeg for reading the manuscript and making valuable suggestions. MSB acknowledges the FAPESP CEPID-Redoxoma grant # 2013/07937-8 and CNPq grant # 303831/2019-7. Itri acknowledges CNPq research fellowship. Itri, Baptista and Franco are grateful to Maressa Donnato for technical supporting in GUVs experiments.

References

[1] M.E. Greenberg, et al., The lipid whisker model of the structure of oxidized cell membranes, J. Biol. Chem. 283 (4) (2008) 2385–2396, https://doi.org/10.1074/jbc.M707348200.
[2] B.G. Halliwell, M.C. John, Free Radical in Biology and Medicine, Oxford Univ. Press, 2015, https://doi.org/10.1093/acprof:oso/9780198717478.001.0001.
[3] A.W. Girotti, Photosensitized oxidation of membrane lipids: reaction pathways, cytotoxic effects, and cytoprotective mechanisms, J. Photochem. Photobiol. B Biol. 63 (1–3) (2001) 103–113, https://doi.org/10.1016/S1011-1344(01)00207-X.
[4] H. Mojzisova, S. Bonneau, P. Maillard, K. Berg, D. Brault, Photosensitizing properties of chlorins in solution and in membrane-mimicking systems, Photochem. Photobiol. Sci. 8 (6) (2009) 778–787, https://doi.org/10.1039/b822269j.
[5] I.O.L. Bacellar, T.M. Tsubone, C. Pavani, M.S. Baptista, Photodynamic efficiency: from molecular photochemistry to cell death, Int. J. Mol. Sci. 16 (9) (2015) 20523–20559, https://doi.org/10.3390/ijms160920523.
[6] I.E. Kochevar, Singlet oxygen signaling: from intimate to global, Sci. STKE 221 (2004) 1–3, https://doi.org/10.1126/stke.2212004pe7.
[7] A.W. Girotti, T. Kriska, Role of lipid hydroperoxides in photo-oxidative stress signaling, Antioxid. Redox Signal. 6 (2) (2004) 301–310, https://doi.org/10.1089/152308604322899369.
[8] A. Reis, C.M. Spickett, Chemistry of phospholipid oxidation, Biochim. Biophys. Acta 1818 (10) (2012) 2374–2387, https://doi.org/10.1016/j.bbamem.2012.02.002.
[9] J. Van Der Paal, E.C. Neyts, A. Bogaerts, Synergistic effect of electric field and lipid oxidation on the permeability of cell membrane, Biochim Biophys Acta - Gen. Subj. 1861 (4) (2017) 839–847, https://doi.org/10.1016/j.bbagen.2017.01.030.
[10] T.T. Tasso, et al., Photobleaching efficiency parallels the enhancement of membrane damage for porphyrazine photosensitizers, J. Am. Chem. Soc. 141 (39) (2019) 15547–15556, https://doi.org/10.1021/jacs.9b05991.
[11] H.W. Gardner, Oxygen radical chemistry of polyunsaturated fatty acids, Free Radic. Biol. Med. 7 (1) (1989) 65–86, https://doi.org/10.1016/0891-5849(89)90102-0.
[12] I.O.L. Bacellar, et al., Photosensitized membrane permeabilization requires contact-dependent reactions between photosensitizer and lipids, J. Am. Chem. Soc. 140 (30) (2018) 9606–9615, https://doi.org/10.1021/jacs.8b05014.
[13] N. Paillous, S. Fery-Forgues, Review interest of photochemical methods for induction of lipid peroxidation, Biochimie 76 (5) (1994) 355–368, https://doi.org/10.1016/0300-9084(94)90109-0.
[14] M. Vignoni, et al., Photooxidation of unilamellar vesicles by a lipophilic pterin: deciphering biomembrane photodamage photodamage, Langmuir 34 (50) (2018) 15578–15586, https://doi.org/10.1021/acs.langmuir.8b03302.
[15] H. Muchalski, A.J. Levonyak, L. Xu, K.U. Ingold, N.A. Porter, Competition H(D) kinetic isotope effects in the autoxidation of hydrocarbons, J. Am. Chem. Soc. 137 (1) (2015) 94–97, https://doi.org/10.1021/ja511434j.
[16] S. Inbar, H. Linschitz, S.G. Cohen, Nanosecond flash studies of reduction of benzophenone by aliphatic amines. Quantum yields and kinetic isotope effects, J. Am. Chem. Soc. 103 (5) (1981) 1048–1054, https://doi.org/10.1021/ja00395a009.
[17] M.S. Shchepinov, Polyunsaturated fatty acid deuteration against neurodegeneration, Trends Pharmacol. Sci. 41 (4) (2020) 236–248, https://doi.org/10.1016/j.tips.2020.01.010.
[18] M.S. Shchepinov, Reactive oxygen species, isotope effect, essential nutrients, and enhanced longevity, Rejuvenation Res. 10 (1) (2007) 47–59, https://doi.org/10.1089/rej.2006.0506.
[19] A.M. Firsov, et al., Threshold protective effect of deuterated polyunsaturated fatty acids on peroxidation of lipid bilayers, FEBS J. 286 (11) (2019) 2099–2117, https://doi.org/10.1111/febs.14807.
[20] X. Wang, P.J. Quinn, The location and function of vitamin E in membranes (Review), Mol. Membr. Biol. 17 (3) (2000) 143–156, https://doi.org/10.1080/09687680010000311.
[21] I.V. Perevoshchikova, D.B. Zorov, Y.N. Antonenko, Peak intensity analysis as a method for estimation of fluorescent probe binding to artificial and natural nanoparticles: Tetramethylrhodamine uptake by isolated mitochondria, Biochim. Biophys. Acta Biomembr. 1778 (10) (2008) 2182–2190, https://doi.org/10.1016/j.bbamem.2008.04.008.
[22] S.T. Hess, S. Huang, A.A. Heikal, W.W. Webb, Biological and chemical applications of fluorescence correlation spectroscopy: a review, Biochemistry 41 (3) (2002) 697–705, https://doi.org/10.1021/bi0118512.
[23] Y. Yorihiro, N. Etsuo, K. Yoshio, S. Hiroyuki, Oxidation of lipids. 7. Oxidation of phosphatidylcholines in homogeneous solution and in water dispersion, Biochim. Biophys. Acta 795 (2) (1984) 332–340.
[24] M.I. Angelova, D.S. Dimitrov, Liposome electroformation, Faraday Discuss. Chem. Soc. 81 (1986) 303–311, https://doi.org/10.1039/DC9868100303.
[25] I.O.L. Bacellar, et al., Permeability of DOPC bilayers under photoinduced oxidation: sensitivity to photosensitizer, Biochim. Biophys. Acta Biomembr. 1860 (11) (2018) 2366–2373, https://doi.org/10.1016/j.bbamem.2018.06.001.
[26] D.V. Chistyakov, et al., Oxylipin profiles as functional characteristics of acute inflammatory responses in astrocytes pre-treated with IL-4, IL-10, or LPS, Int. J. Mol. Sci. 21 (5) (2020) 1–14, https://doi.org/10.3390/ijms21051780.
[27] W. Caetano, et al., Photo-induced destruction of giant vesicles in methylene blue solutions, Langmuir 23 (3) (2007) 1307–1314, https://doi.org/10.1021/la061510v.
[28] J. Heuvingh, S. Bonneau, Asymmetric oxidation of giant vesicles triggers curvature-associated shape transition and permeabilization, Biophys. J. 97 (11) (2009) 2904–2912, https://doi.org/10.1016/j.bpj.2009.08.056.
[29] K.A. Riske, et al., Giant vesicles under oxidative stress induced by a membrane-anchored photosensitizer, Biophys. J. 97 (5) (2009) 1362–1370, https://doi.org/10.1016/j.bpj.2009.06.023.
[30] P. Boonnoy, V. Jarerattanachat, M. Karttunen, J. Wong-ekkabut, Bilayer deformation, pores, and micellation induced by oxidized lipids, J. Phys. Chem. Lett. 6 (24) (2015) 4884–4888, https://doi.org/10.1021/acs.jpclett.5b02405.
[31] G. Weber, et al., Lipid oxidation induces structural changes in biomimetic membranes, Soft Matter 10 (24) (2014) 4241–4247, https://doi.org/10.1039/c3sm52740a.
[32] A. Bour, S.G. Kruglik, M. Chabanon, P. Rangamani, N. Puff, S. Bonneau, Lipid unsaturation properties govern the sensitivity of membranes to photoinduced oxidative stress, Biophys. J. 116 (5) (2019) 910–920, https://doi.org/10.1016/j.bpj.2019.01.033.
[33] N.M. Shalene Sankhagowit, Wu Shao-Hua, Roshni Biswas, Carson T. Riche, Michelle L. Povinelli, The dynamics of giant unilamellar vesicle oxidation probed by morphological transitions, Biochim. Biophys. Acta Biomembr. 1838 (10) (2014) 2615–2624, https://doi.org/10.1016/j.bbamem.2014.06.020.
[34] H. Khandelia, O.G. Mouritsen, Lipid gymnastics: evidence of complete acyl chain reversal in oxidized phospholipids from molecular simulations, Biophys. J. 96 (7) (2009) 2734–2743, https://doi.org/10.1016/j.bpj.2009.01.007.
[35] Y. Sakuma, T. Taniguchi, M. Imai, Pore formation in a binary giant vesicle induced by cone-shaped lipids, Biophys. J. 99 (2) (2010) 472–479, https://doi.org/10.1016/j.bpj.2010.03.064.
[36] T.I. Rokitskaya, M. Block, Y.N. Antonenko, E.A. Kotova, P. Pohl, Photosensitizer binding to lipid bilayers as a precondition for the photoinactivation of membrane channels, Biophys. J. 78 (5) (2000) 2572–2580, https://doi.org/10.1016/S0006-3495(00)76801-9.
[37] A.A. Pashkovskaya, E.A. Sokolenko, V.S. Sokolov, E.A. Kotova, Y.N. Antonenko, Photodynamic activity and binding of sulfonated metallophthalocyanines to phospholipid membranes: contribution of metal-phosphate coordination, Biochim. Biophys. Acta Biomembr. 1768 (10) (2007) 2459–2465, https://doi.org/10.1016/j.bbamem.2007.05.018.

[38] G.J. Bachowski, E. Ben-Hur, A.W. Girotti, Phthalocyanine-sensitized lipid peroxidation in cell membranes: use of cholesterol and azide as probes of primary photochemistry, J. Photochem. Photobiol. B Biol. 9 (3–4) (1991) 307–321, https://doi.org/10.1016/1011-1344(91)80168-H.
[39] D.A. Singleton, C. Hang, 13C and 2H kinetic isotope effects and the mechanism of Lewis acid- catalyzed ene reactions of formaldehyde, J. Organomet. Chem. 65 (3) (2000) 895–899, https://doi.org/10.1021/jo9917590.
[40] D.A. Singleton, C. Hang, M.J. Szymanski, E.E. Greenwald, A new form of kinetic isotope effect. Dynamic effects on isotopic selectivity and regioselectivity, J. Am. Chem. Soc. 125 (5) (2003) 1176–1177, https://doi.org/10.1021/ja027221k.
[41] V.B. Luzhkov, Theoretical study of deuterium kinetic isotope effect in peroxidation of phenol and toluene, Chem. Phys. 320 (1) (2005) 1–8, https://doi.org/10.1016/j.chemphys.2005.06.011.
[42] Urano Shiro, Yano Keiko, Mitsuyoshi Matsuo, Membrane-stabilizing effect of vitamin E: effect of α-tocopherol and its model compounds on fluidity of lecithin liposomes, Biochem. Biophys. Res. Commun. 150 (1) (1988) 469–475.
[43] V.W. Bowry, R. Stocker, Tocopherol-mediated peroxidation. The prooxidant effect of vitamin E on the radical-initiated oxidation of human low-density lipoprotein, J. Am. Chem. Soc. 115 (14) (1993) 6029–6044, https://doi.org/10.1021/ja00067a019.
[44] P. Boonnoy, M. Karttunen, J. Wong-Ekkabut, Alpha-tocopherol inhibits pore formation in oxidized bilayers, Phys. Chem. Chem. Phys. 19 (8) (2017) 5699–5704, https://doi.org/10.1039/C6CP08051K.
[45] V.W. Bowry, K.U. Ingold, The unexpected role of vitamin E (α-tocopherol) in the peroxidation of human low-density lipoprotein, Acc. Chem. Res. 32 (1) (1999) 27–34, https://doi.org/10.1021/ar950059o.
[46] K. Fukuzawa, Y. Inokami, A. Tokumura, J. Terao, A. Suzuki, Singlet oxygen scavenging by α-tocopherol and β-carotene: kinetic studies in phospholipid membranes and ethanol solution, BioFactors 7 (1–2) (1998) 31–40, https://doi.org/10.1002/biof.5520070106.
[47] A.M. Firsov, E.A. Kotova, E.A. Korepanova, A.N. Osipov, Y.N. Antonenko, Peroxidative permeabilization of liposomes induced by cytochrome c/cardiolipin complex, Biochim. Biophys. Acta Biomembr. 1848 (3) (2015) 767–774, https://doi.org/10.1016/j.bbamem.2014.11.027.
[48] A.I. Sorochkina, S.I. Kovalchuk, E.O. Omarova, A.A. Sobko, E.A. Kotova, Y. N. Antonenko, Peptide-induced membrane leakage by lysine derivatives of gramicidin a in liposomes, planar bilayers, and erythrocytes, Biochim. Biophys. Acta Biomembr. 1828 (11) (2013) 2428–2435, https://doi.org/10.1016/j.bbamem.2013.06.018.
[49] Y.N. Antonenko, A.S. Lapashina, E.A. Kotova, A.A. Ramonova, M.M. Moisenovich, I.I. Agapov, Application of peak intensity analysis to measurements of protein binding to lipid vesicles and erythrocytes using fluorescence correlation spectroscopy: dependence on particle size, J. Membr. Biol. 250 (1) (2017) 77–87, https://doi.org/10.1007/s00232-016-9938-6.
[50] O. Krichevsky, G. Bonnet, Fluorescence correlation spectroscopy: the technique and its applications, Rep. Prog. Phys. 65 (2002) 251–297, https://doi.org/10.1007/978-1-59745-513-8_7.
[51] R. Shimizu, M. Yagi, A. Kikuchi, Suppression of riboflavin-sensitized singlet oxygen generation by L-ascorbic acid, 3-O-ethyl-L-ascorbic acid and Trolox, J. Photochem. Photobiol. B Biol. 191 (2019) 116–122, https://doi.org/10.1016/j.jphotobiol.2018.12.012.
[52] A.Y. Andreyev, et al., Isotope-reinforced polyunsaturated fatty acids protect mitochondria from oxidative stress, Free Radic. Biol. Med. 82 (2015) 63–72, https://doi.org/10.1016/j.freeradbiomed.2014.12.023.
[53] C.R. Lamberson, et al., Unusual kinetic isotope effects of deuterium reinforced polyunsaturated fatty acids in tocopherol-mediated free radical chain oxidations, J. Am. Chem. Soc. 136 (3) (2014) 838–841, https://doi.org/10.1021/ja410569g.
[54] S. Hill, et al., Small amounts of isotope-reinforced polyunsaturated fatty acids suppress lipid autoxidation, Free Radic. Biol. Med. 53 (4) (2012) 893–906, https://doi.org/10.1016/j.freeradbiomed.2012.06.004.
[55] M.S. Baptista, J. Cadet, A. Greer, A.H. Thomas, Photosensitization reactions of biomolecules: definition, targets and mechanisms, Photochem. Photobiol. 97 (6) (2021) 1456–1483, https://doi.org/10.1111/php.13470.
[56] J.D. Spikes, Phthalocyanines as photosensitizers in biological systems and for the photodynamic therapy of tumors, Photochem. Photobiol. 43 (6) (1986) 691–699.
[57] I. Rosenthal, Phthalocyanines as photodynamic sensitizer, Photochem. Photobiol. 53 (6) (1991) 859–870.
[58] A. Pashkovskaya, et al., Light-triggered liposomal release: membrane permeabilization by photodynamic action, Langmuir 26 (8) (2010) 5725–5733, https://doi.org/10.1021/la903867a.
[59] V.L. Shapovalov, T.I. Rokitskaya, E.A. Kotova, O.V. Krokhin, Y.N. Antonenko, Effect of fluoride anions on gramicidin Photoinactivation sensitized by sulfonated aluminum phthalocyanines, Photochem. Photobiol. 74 (1) (2001) 1–7, https://doi.org/10.1562/0031-8655(2001)0740001EOFAOG2.0.CO2.
[60] P. Pearson, S.A. Lewis, J. Britton, I.S. Young, A. Fogarty, The pro-oxidant activity of high-dose vitamin E supplements in vivo, BioDrugs 20 (5) (2006) 271–273, https://doi.org/10.2165/00063030-200620050-00002.
[61] J.M. Upston, P.K. Witting, R. Alleva, R. Stocker, Oxidation of free fatty acids in low density lipoprotein by 15-lipoxygenase stimulates nonenzymic, α-tocopherol-mediated peroxidation of cholesteryl esters, J. Biol. Chem. 272 (48) (1997) 30067–30074.
[62] Y. Yoshida, A. Umeno, Y. Akazawa, M. Shichiri, Chemistry of lipid peroxidation products and their use as biomarkers in early detection of diseases, J. Oleo Sci. 64 (4) (2015) 347–356.
[63] V. Vangaveti, B.T. Baune, R.L. Kennedy, Hydroxyoctadecadienoic acids: novel regulators of macrophage differentiation and atherogenesis, Ther. Adv. Endocrinol. Metab. 2 (1) (2010) 51–60, https://doi.org/10.1177/2042018810375656.
[64] I.O.L. Bacellar, M.S. Baptista, Mechanisms of photosensitized lipid oxidation and membrane permeabilization, ACS Omega 4 (26) (2019) 21636–21646, https://doi.org/10.1021/acsomega.9b03244.
[65] Hugh Davison, J.F. Danielli, The permeability of natural membranes, Cambridge 118 (3055) (1952) 90, https://doi.org/10.1126/science.118.3055.90.b.
[66] J.T. Brenna, et al., Plasma and red blood cell membrane accretion and pharmacokinetics of RT001 (bis -allylic 11, 11-D2-Linoleic Acid Ethyl Ester) during long term dosing in patients, J. Pharm. Sci. 109 (11) (2020) 3496–3503, https://doi.org/10.1016/j.xphs.2020.08.019.
[67] M.S.S.Y. Liu, B.A. Bell, Y. Song, K. Zhang, B. Anderson, P.H. Axelsen, W. Bohannan, M.-P. Agbaga, H.G. Park, G. James, J.T. Brenna, K. Schmidt, J.L. Dunaief, Deuterated docosahexaenoic acid protects against oxidative stress and geographic atrophy-like retinal degeneration in a mouse model with iron overload, Aging Cell 00:e13579 (2022), https://doi.org/10.1111/acel.13579. In press.
[68] M.S. Shchepinov, et al., Deuterium protection of polyunsaturated fatty acids against lipid peroxidation: a novel approach to mitigating mitochondrial neurological diseases, Omega-3 Fat. Acids Brain Neurol. Heal. (2014) 373–383, https://doi.org/10.1016/B978-0-12-410527-0.00031-4.
[69] W.S. Yang, B.R. Stockwell, Ferroptosis: death by lipid peroxidation, Trends Cell Biol. 26 (3) (2016) 165–176, https://doi.org/10.1016/j.tcb.2015.10.014.
[70] M.G. Cotticelli, A.M. Crabbe, R.B. Wilson, M.S. Shchepinov, Insights into the role of oxidative stress in the pathology of friedreich ataxia using peroxidation resistant polyunsaturated fatty acids, Redox Biol. 1 (1) (2013) 398–404, https://doi.org/10.1016/j.redox.2013.06.004.
[71] P.R. Angelova, M.H. Horrocks, D. Klenerman, S. Gandhi, A.Y. Abramov, M. S. Shchepinov, Lipid peroxidation is essential for α-synuclein-induced cell death, J. Neurochem. 133 (4) (2015) 582–589, https://doi.org/10.1111/jnc.13024.
[72] A. Hatami, et al., Deuterium-reinforced linoleic acid lowers lipid peroxidation and mitigates cognitive impairment in the Q140 knock in mouse model of Huntington ‘s disease, FEBS J. 285 (16) (2018) 3002–3012, https://doi.org/10.1111/febs.14590.
[73] S.M. Raefsky, R. Furman, G. Milne, E. Pollock, P. Axelsen, M.P. Mattson, M. S. Shchepinov, Deuterated polyunsaturated fatty acids reduce brain lipid peroxidation and hippocampal amyloid β-peptide levels, without discernable behavioral effects in an APP/PS1 mutant transgenic mouse model of Alzheimer’s disease, Neurobiol. Aging 66 (2019) 165–176, https://doi.org/10.1016/j.neurobiolaging.2018.02.024.Deuterated.
[74] T. Zesiewicz, et al., Randomized, clinical trial of RT001: early signals of efficacy in Friedreich’s ataxia, Mov. Disord. 33 (6) (2018) 1000–1005, https://doi.org/10.1002/mds.27353.
[75] P.R. Allen, T.M. Cullis, Liposomal drug delivery systems: from concept to clinical applications, Adv. Drug Deliv. Rev. 65 (1) (2013) 36–48, https://doi.org/10.1016/j.addr.2012.09.037.